Tuning the Aggregates of Thiophene-based Trimers by Methyl Side-chain Engineering for Photocatalytic Hydrogen Evolution

Xiaojiao Yuan, Kunran Yang, Chloé Grazon, Cong Wang, Lorenzo Vallan, Jean-David Isasa, Pedro Resende, Fanxing Li, Cyril Brochon, Hynd Remita, et al.

Tuning the Aggregates of Thiophene-based Trimers by Methyl Side-chain Engineering for Photocatalytic Hydrogen Evolution

Xiaojiao Yuan, *[a] Kunran Yang, [b] Chloé Grazon, [c] Cong Wang, [d] Lorenzo Vallan, [a] Jean-David Isasa, [a] Pedro M. Resende, [a] Fanxing Li, [b] Cyril Brochon, [a] Hynd Remita, [d] Georges Hadziioannou, [a] Eric Cloutet, *[a] Jian Li *[d], [e]

[a] Dr. X. Yuan, Dr. L. Vallan, Dr. P. M. Resende, J.-D. Isasa, Dr. C. Brochon, Dr. G. Hadziioannou, Dr. E. Cloutet
Université de Bordeaux, CNRS, Bordeaux INP, LCPO, UMR5629, Allée Geoffroy Saint Hilaire, Bâtiment B8, F-33607 Pessac, France
E-mail: yxjxjks@126.com; eric.cloutet@u-bordeaux.fr;

[b] Dr. K. Yang, Dr. F. Li
Department of Chemical and Biomolecular Engineering, North Carolina State University
Raleigh, NC 27695-7905, USA

[c] Dr. C. Grazon
Univ. Bordeaux, CNRS, Bordeaux INP, ISM, UMR 5255, F-33400 Talence, France

[d] Dr. C. Wang, Dr. H. Remita, Dr. J. Li
Institut de Chimie Physique, UMR 8000 CNRS, Université Paris-Saclay
310 Rue Michel Magat, 91400 Orsay, France

[e] Dr. J. Li
Laboratory of Renewable Energy Science and Engineering, École Polytechnique Fédérale de Lausanne (EPFL), Switzerland
E-mail: jian.li@epfl.ch

X. Yuan and K. Yang contribute equally to this work

Supporting information for this article is given via a link at the end of the document.

Abstract: Organic π-conjugated semiconductors (OCSs) have recently emerged as a promising alternative to traditional inorganic materials for photocatalysis. However, the aggregation of OCSs in photocatalytic aqueous solution caused by self-assembly, which closely relates to the photocatalytic activity, has not yet been studied. Here, the relationship between the aggregation of 4,7-Bis(thiophen-2-yl) benzothiadiazole (TBT) and the photocatalytic activity was systematically investigated by introducing

and varying the position of methyl side chains on the two peripheral thiophene units. Experimental and theoretical results indicated that the introduction of -CH_3 group at the 3-position of TBT resulted in the smallest size and best crystallinity of aggregates compared to that of TBT, 4- and 5-positions. As a result, TBT-3 exhibited an excellent photocatalytic activity towards H_2 evolution, ascribed to the shorten charge carrier transport distance and solid long-range order. These results suggest the important role of aggregation behavior of OCSs for efficient photocatalysis.

Keywords: Aggregation • Intramolecular packing • Thiophene • Photocatalysis • Hydrogen Production

Introduction

Organic π-conjugated semiconductors (OCSs) with tunable energy levels, excellent chemical stability and broad absorption, have triggered a huge interest in photocatalysis.[1] Substantial efforts such as molecule design, structure regulation and side-chain engineering have recently been invested to improve the photocatalytic performance of OCSs by fine-tuning optical property, band energy levels and conductivity.[2] Because of the insolubility in aqueous solution and intermolecular non-covalent interactions (such as electrostatic, hydrophobic, and π-π stacking), OCSs usually exhibit distinct aggregation characteristics in aqueous photocatalytic solution, i.e., self-assemble to form nano- or micro-agglomerates.[3] Therefore, the entire photocatalytic process including generation, separation and migration of photogenerated carriers, takes place in aggregates instead of individual organic molecules. On one hand, the size of aggregates, which determines both the number of surface-active sites in term of specific surface area and the transportation distance of electrons to the surface, has a remarkable influence on the photocatalytic performance.[4] On the other hand, the crystallinity of the aggregates critically affects the intrinsic charge separation and transport. A higher crystallinity with fewer recombination centers facilitates more photogenerated charge carrier to diffuse from the bulk to surface for redox reactions. Therefore, judiciously engineering the intramolecular packing to regulate the size and crystallinity of aggregates is essential to achieve efficient photocatalytic performance for OSCs.

Side-chain engineering is an effective strategy to fine-tune the intramolecular packing and crystallinity by alteration of chain length, branching position and size of the branched alkyl chains.[5] [6], [7] In this work, methyl groups (-CH_3), as the smallest alkyl substitution unit, with minimal competition for space-filling, were selected as side chain groups, which can effectively avoid side chain entanglement caused by long side chain, thus reducing the interference of other factors. Thiophene-based conjugated

trimers with donor-acceptor-donor (D-A-D) molecule structure were prepared as an OCS model because the strong intermolecular interactions generated by the D-A moiety favor the self-organization of trimers into ordered structures and close packing with increasing π-π orbital overlap.[8] The relationships of aggregation-property-activity was systematically studied by introducing -CH_3 side chain on different positions of TBT. 4,7-bis(3-methylthiophen-2-yl)benzo[c][1,2,5]thiadiazole (TBT-3) which possesses larger steric hindrance than TBT, 4,7-bis(4-methylthiophen-2-yl)benzo[c][1,2,5]thiadiazole (TBT-4) and 4,7-bis(5-methylthiophen-2-yl)benzo[c][1,2,5]thiadiazole (TBT-5) showed the smallest size and the best crystallinity. The smaller aggregates and favorable crystalline properties contribute to the solid long-range order and charge carrier transport of TBT-3, leading to a superior photocatalytic activity for hydrogen production. DFT calculations demonstrated that TBT-3 maintained weak aggregation ability, which enables the reaction on a larger surface area; TBT-3 also exhibited reactive molecular orbitals, making it favorable for hydrogen evolution. The deep understanding of the relationship between the aggregation and photocatalytic activity can provide important insight in design of OCSs for efficient photocatalytic fuel production.

Results and Discussion

The D-A-D conjugated trimers (TBT) were synthesized by Pd (0)-catalyzed Suzuki-Miyaura cross-coupling and Stille cross-coupling reactions (**Figure 1a and Schemes S1-S4**), in which thiophene (T) and benzothiadiazole (B) serve as electron donor and acceptor, respectively. (**Figure S1**). The chemical structures of these purified trimers were confirmed by ^{1}H NMR, ^{13}C NMR, mass spectrometry, elemental analysis and single crystal X-ray diffraction (**Figure S2-S10, Table S1**). All the prepared trimers are fully soluble in common organic solvents such as dichloromethane, tetrahydrofuran (THF), acetone, dimethyl sulfoxide (DMSO) and ethanol, but insoluble in water, which thus results in the formation of aggregates in aqueous photocatalytic system (H_2O/TEOA = 9: 1, v/v). Obviously, TBT-3 presented the best dispersion compared with TBT-4, TBT-5 and TBT (**Figure 1b**). The aggregates size of the trimers in H_2O/TEOA solution was further measured by dynamic light scattering (DLS). Compared to TBT (~400 nm), TBT-4 (~1.2 μm) and TBT-5 (~1.3 μm), TBT-3 exhibited the smallest aggregates size with the average dimeter of ~50 nm (**Figure 1c and Figure S11**). The similar surface tension for all the samples suggests that the aggregates size is not dominated by the surface tension (**Figure S12**). Compared to TBT, a blue shift of absorption and emission wavelengths was observed for TBT-3 while a red shift was obtained for TBT-4 and TBT-5 (**Figure 1d and Figure S13**), consistent with the simulated results (**Figure**

S14). The different absorption shifts of these trimers indicate that the position of the side chains affect the photophysical properties.[5a, 9]

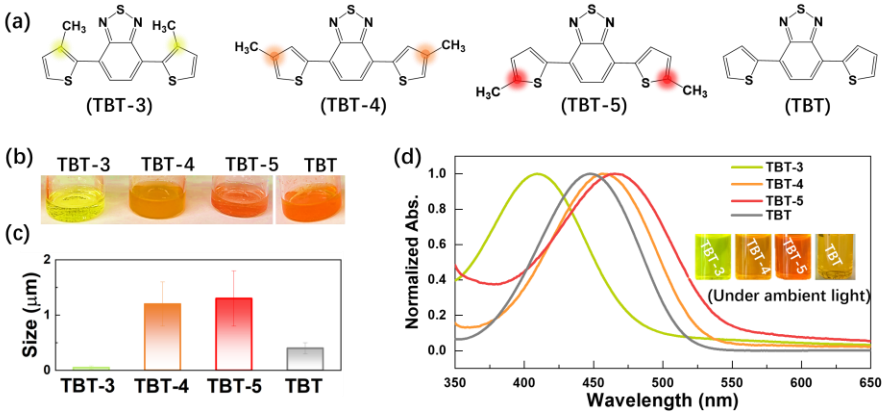

Figure 1. (a) Chemical structures of conjugated trimers and (b) Photographs of the trimer samples in THF/H_2O/TEOA solution; (c) DLS measurement of trimer aggregates; (d) Normalized UV-Vis absorption spectra of catalysts dissolved in THF and photograph of catalysts in THF solution under ambient light (insert images);

Transmission electron microscopy (TEM) was used to characterize the morphology of the prepared TBT-based trimers. All of these trimers exhibited rod-like structures (**Figure 2a-i and Figure S15-16**). The EDS (Energy Dispersive Spectroscopy) diagram showed that the trimers only contained S and C elements without additional Pd. The absence of Pd signal in inductively coupled plasma-mass spectrometry (ICP-MS) and X-ray photoelectron spectroscopy (XPS) further confirmed the extremely low amount residual Pd in the samples (**Figure S17, Table S2**). Raman spectra was used to characterize the chemical structure of the prepared trimers. The strong peaks around 1377 cm^{-1} and 1419 cm^{-1} correspond to the C-C and C=C stretches, respectively, on the bridging thiophene units. The peaks in the range 1324-1360 cm^{-1} and the peak at 1538 cm^{-1} correspond to the C-C bands and ring stretch in B unit, respectively.[10] Furthermore, the increased steric hindrance caused by the side chain led to some peaks splitting into two components. Similar phenomenon also occurs in previous research in regio-random P3HT.[10a] Differential scanning calorimetry (DSC), X-ray powder diffraction (XRD), and thermogravimetric analysis (TGA) revealed that all the trimers possess good crystallinity and thermal stability (**Figure 2n**, **Figure S18-19**). The diffuse rings in two-dimensional (2D) scattering pattern maps indicated that the crystals were randomly oriented (**Figure 2o**) and all the trimers were 2D hexagonal structures based on the peak position of (100) Bragg reflection (**Figure S20**). Unlike TBT-3, a wide peak appeared in the pattern of TBT, TBT-4 and TBT-5, which suggested the presence of an amorphous phase

in TBT, TBT-4 and TBT-5 **(Figure 2p)**. The crystalline fraction for TBT-3 was further determined to be 88.1%, which was much higher than that of TBT (65.1%), TBT-4 (74.6%) and TBT-5 (70.0%) (**Figure S21**). Evidently, TBT-3 displayed the best crystallinity compared with TBT-4, TBT-5 and TBT, possibly due to the enhanced steric hinderance which prevent the tight packing of molecules and increase the intermolecular spacing, leading to an improved crystallinity.[11] Therefore, the introduction of methyl side-chains at the 3-position of TBT improves the crystalline properties, which contribute to solid long-range order and charge carriers' transport in photocatalysis.[8a, 12]

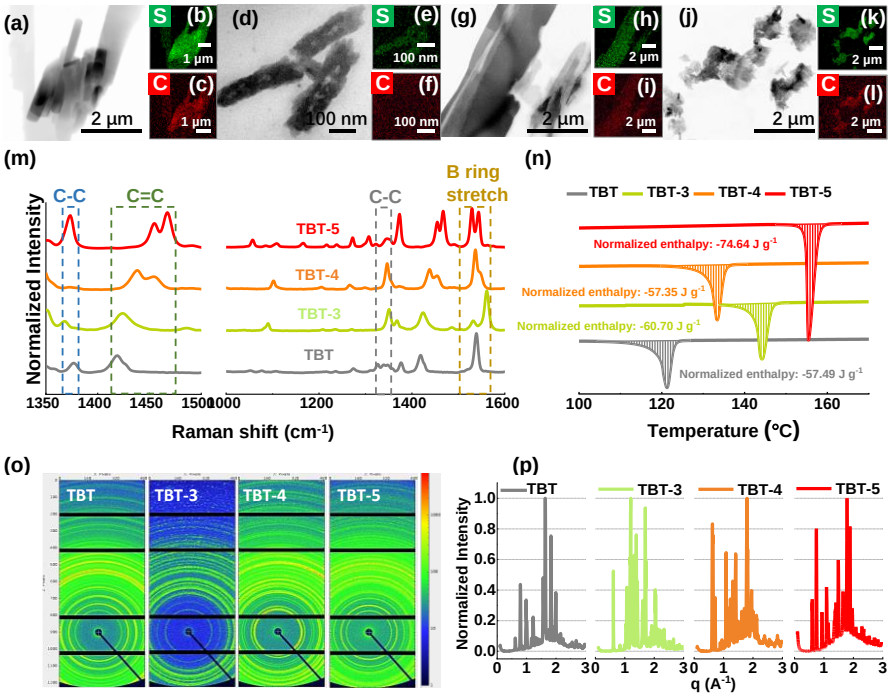

Figure 2. TEM images and element mappings of TBT (a-c), TBT-3 (d-f), TBT-4 (g-i) and TBT-5 (j-l); (m) Raman spectra for the trimers; (n) DSC measurement of the trimers; (o) the WAXS 2D pattern and (p) WAXS spectra for the as-prepared trimers.

The optical absorption properties of the solid trimers were investigated by UV-Vis diffuse reflectance spectroscopy (DRS) and simulated DFT calculations. The results showed that all the trimers exhibit broad light absorption (**Figure 3a and Figure S22**). Notably, different stacking modes in the solid state contribute differently to the absorption properties.[3, 13] TBT-5 and TBT show red-shifted absorption compared to that of TBT-3 and TBT-4, which may be ascribed to more planar backbone of TBT and TBT-5.[14] The optical band gaps (E_g) of the trimers were calculated and found to be 2.32 eV (TBT-3), 2.17 eV (TBT-4), 2.04 eV (TBT) and 1.99 eV (TBT-5) from the Tauc plots (**Figure 3b**). The HOMO (highest occupied molecular orbital) and LUMO (lowest unoccupied molecular orbital) energy levels of

trimers were determined by electrochemical cyclic voltammetry (**Figure 3c-d and Figure S23**). The HOMO/LUMO energy levels of TBT, TBT-3, TBT-4 and TBT-5 were calculated to be 0.77/-1.27 eV, 0.98/-1.34 eV, 0.93/-1.24 eV and 0.73/-1.26 eV, respectively, according to the equations: E_{LUMO} = -e [E_{red} - $E_{(Fc/Fc+)}$ + 4.8] eV and E_{HOMO} = E_g - E_{LUMO}. All the trimers are thermodynamically suitable for driving the reduction of protons to H_2 due to their more negative reduction potential than the reduction of proton. The smallest semicircle in a Nyquist plot for TBT-3 demonstrated a better charge transfer ability than TBT, TBT-4 and TBT-5 (**Figure 3e**).

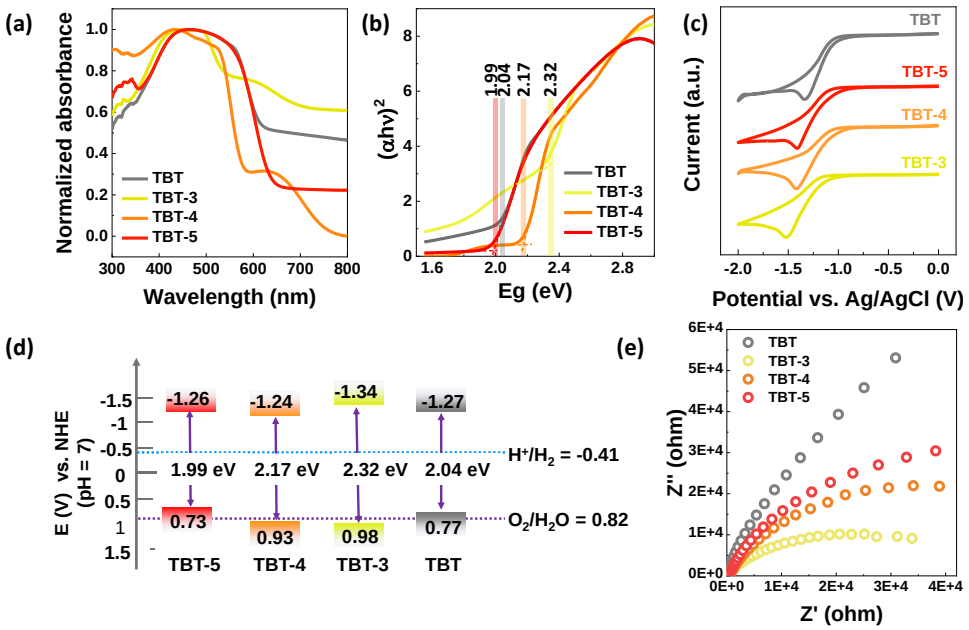

Figure 3. (a) DRS absorption spectra of the samples measured in the solid state (intensities normalized); (b) Calculated band gaps from the Tauc plots; (c) Cyclic voltammetry plots (reduction scans) of trimers in acetonitrile solution and 0.1 M tetrabutylammonium perchlorate; (d) Experimentally determined HOMO and LUMO energy levels of samples; (e) Nyquist plot of TBT, TBT-3, TBT-4, and TBT-5.

As discussed above, photocatalytic process takes place in aggregates instead of individual organic molecules, (**Figure 4a)**. The photocatalytic hydrogen production of the prepared trimers was investigated in TEOA/H_2O (V_{TEOA}/V_{H2O} = 1: 9) solution without any cocatalysts modification under both UV-Vis light ($\lambda \geq 360$ nm) and visible light ($\lambda \geq 420$ nm) irradiation. No hydrogen was measured without trimers in the solution or under dark conditions. Large amounts of H_2 were produced for all the trimers under UV and visible light illumination (**Figure 4b-c, Table S3**). Due to the electron donating effect of the alkyl group, TBT-3, TBT-4 and TBT-5 presented higher H_2 production than TBT. TBT-3 displayed the best activity although it has larger band gap and blue-shifted absorption compared to TBT-4 and TBT-5, which

was attributed to its better crystalline properties and smaller aggregation size. It should be noted that the activity of TBT-3 was comparable to other OCSs even without cocatalyst and residual Pd (**Table S4**). The photocatalytic stability of the TBT-3 was also tested, and no obvious change was observed during 25 h test (**Figure 4d**). FTIR analysis of the recycled TBT-3 revealed the high stability of its chemical structure and composition after photocatalytic tests (**Figure S24**). To further study the dynamics of photo-excited carriers of the aggregates, transient absorption spectroscopy (TAS) was carried out (**Figure S25**). Notably, the charge-transfer signal in TBT-3 was much more pronounced and persisted for a longer timescale than that in TBT, TBT-4 and TBT-5. The lifetime was estimated to be ~1.2 ns, which possibly reflects the fewer structural defects in TBT-3 which effectively decelarate the charge trapping and recombination. These results demonstrated that the smaller size and higher crystallinity of TBT-3 enabled it with much enhanced charge carrier dynamics, which possibly promotes the light-driven electron transfer from aggregates to bulk solvent for H_2 production.[15]

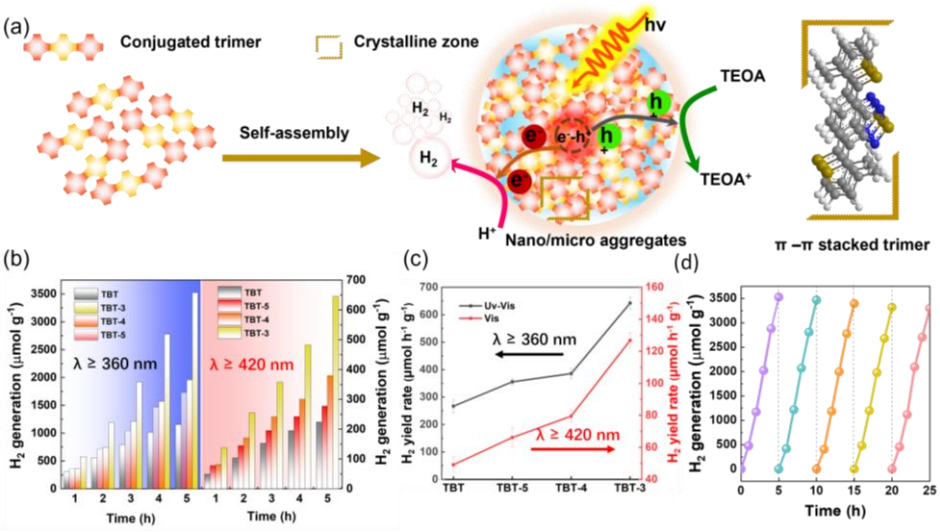

Figure 4. (a) Probable mechanism for the formation of microaggregates and the photocatalytic mechanism. (b) Time course of photocatalytic H_2 generation for aggregates under UV-Vis and visible light ($\lambda \geq 420$ nm) irradiation; (c) Normalized H_2 production under UV-Vis light. Time-course of photocatalytic H_2 generation for trimers under visible light and visible light; (d) H_2 generation with cycling**.**

Density functional theory (DFT) was further employed to provide molecular-level understanding on these trimers. **Figure 5a** showed the energy change (ΔE) of the aggregation process from separated molecules. Compared with TBT, TBT-4 and TBT-5, TBT-3 released the smallest amount of energy, suggesting that the TBT-3 had the lowest tendency to aggregate. In addition to the aggregates, the energy

change for the formation of crystal structures from separated molecules was also determined (**Figure S26**). The ΔE of forming the crystal structures of TBT-3, TBT-4 and TBT-5 were -1.04 eV, -1.20 eV and -1.14 eV per molecule, respectively, consistent with the trend in Figure 5a. The smaller aggregate size of TBT-3 created a smaller reaction platform for HER, which facilitates the reaction on a larger specific surface area and shortens the transportation distance of photogenerated carriers to the surface of the aggregates. The decreased thermodynamic driving force for aggregation of TBT-3 was further confirmed by the lower densities of TBT-3 crystals (**Figure 5d**). In addition, the calculated HOMO-LUMO gaps are generally consistent with the optical gaps determined experimentally (**Figure 5b**). Despite the large HOMO-LUMO gap of TBT-3, TBT-3 exhibited a superior activity as indicated from its large density of electrons at the HOMO state (**Figure S27**). Electrons are mainly distributed around the S atoms of the thiophen- group and the N atoms of the thiadiazole- group at both ground and excited states, indicating the existence of intramolecular charge transfer **(Figure 5c)**. In addition, there is an obvious structural deformation at the thiophen side groups after excitation due to the largest steric hindrance effect of TBT-3, which will also contribute to the charge transfer by forming a larger π-conjugated region. In summary, the decreased aggregation tendency of TBT-3 leads to a smaller aggregate size, and its reactive molecular orbitals strongly enhance the photocatalytic HER, which is responsible for the higher H_2 production of TBT-3.

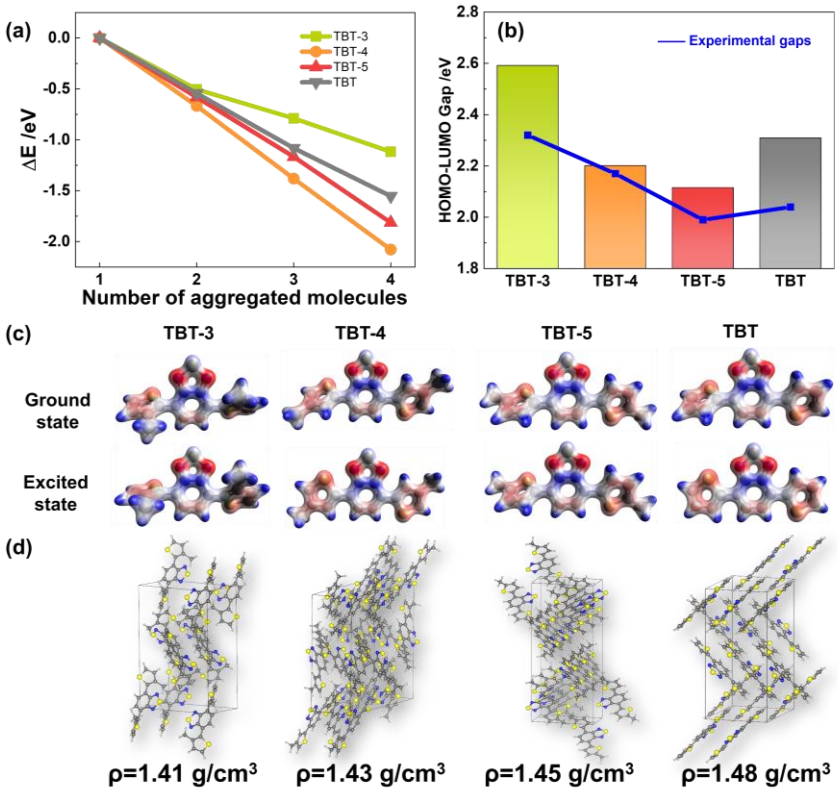

Figure 5. (a) Energy change of aggregating different number of molecules. (b) Calculated HOMO-LUMO gap and the experimental determined gaps for the considered molecules. (c) Electron density distribution of TBT-3, TBT-4, TBT-5 and TBT at ground state and excited state (d) Optimized structures and corresponding densities of TBT-3, TBT-4, TBT-5 and TBT.

Conclusion

In summary, the aggregation size and crystallization properties of TBT were successfully regulated by incorporating and alternating the position of methyl side chains on thiophene units. The introduction of -CH_3 at the 3-position of TBT not only increased the crystallinity, but also reduces the degree of agglomeration, which in turn reduced the distance for electrons to migrate to the surface and improved the charge transportation performance, resulting in an enhanced photocatalytic activity. These results demonstrated that the aggregation behavior and crystalline state of OSCs can be effectively tuned by the subtle manipulation of side chain, which opens a new avenue for the design of high-performance OCSs photocatalysts for solar fuels production.

Acknowledgements

X. Yuan gratefully acknowledges the financial support for postdoctoral research by European Union's Horizon 2020 research and innovation program under the grant agreement No.800926 (HyPhOE). Catherine Denage (ICMCB-UMR5026) is acknowledged for the ICP-OES measurement. We acknowledge Sabrina Lacomme for the TEM measurements (Bordeaux Imaging Center-Imagerie Electronique, Université de Bordeaux, 33076 Bordeaux Cedex).

Reference

[1] aC. Dai, B. Liu, *Energy & Environmental Science* **2020**, *13*, 24-52; bY. Xiang, X. Wang, L. Rao, P. Wang, D. Huang, X. Ding, X. Zhang, S. Wang, H. Chen, Y. Zhu, *ACS Energy Letters* **2018**, *3*, 2544-2549; cW. Huang, Q. He, Y. Hu, Y. Li, *Angewandte Chemie* **2019**, *131*, 8768-8772; dG. Zhang, Z. A. Lan, X. Wang, *Angewandte Chemie International Edition* **2016**, *55*, 15712-15727; eL. Li, Z. Cai, Q. Wu, W.-Y. Lo, N. Zhang, L. X. Chen, L. Yu, *Journal of the American Chemical Society* **2016**, *138*, 7681-7686; fZ. A. Lan, G. Zhang, X. Chen, Y. Zhang, K. A. Zhang, X. Wang, *Angewandte Chemie International Edition* **2019**, *58*, 10236-10240; gJ. Li, X. Gao, L. Zhu, M. N. Ghazzal, J. Zhang, C.-H. Tung, L.-Z. Wu, *Energy & Environmental Science* **2020**, *13*, 1326-1346;

hJ. Li, X. Han, D. Wang, L. Zhu, M. H. Ha-Thi, T. Pino, J. Arbiol, L. Z. Wu, M. Nawfal Ghazzal, *Angewandte Chemie* **2022**, *134*, e202210242; iX. Yuan, C. Wang, D. Dragoe, P. Beaunier, C. Colbeau-Justin, H. Remita, *Applied Catalysis B: Environmental* **2021**, *281*, 119457; jX. Yuan, D. Dragoe, P. Beaunier, D. B. Uribe, L. Ramos, M. G. Méndez-Medrano, H. Remita, *Journal of Materials Chemistry A* **2020**, *8*, 268-277.

[2] H. Yang, C. Li, T. Liu, T. Fellowes, S. Y. Chong, L. Catalano, M. Bahri, W. Zhang, Y. Xu, L. Liu, *Nature Nanotechnology* **2023**, 1-9.

[3] M. Más-Montoya, R. A. Janssen, *Advanced Functional Materials* **2017**, *27*, 1605779.

[4] H. Wang, X. Liu, P. Niu, S. Wang, J. Shi, L. Li, *Matter* **2020**, *2*, 1377-1413.

[5] aG. Chai, Y. Chang, J. Zhang, X. Xu, L. Yu, X. Zou, X. Li, Y. Chen, S. Luo, B. Liu, *Energy & Environmental Science* **2021**; bD. J. Woods, S. A. Hillman, D. Pearce, L. Wilbraham, L. Q. Flagg, W. Duffy, I. McCulloch, J. R. Durrant, A. A. Guilbert, M. A. Zwijnenburg, *Energy & Environmental Science* **2020**, *13*, 1843-1855; cZ. Hu, Z. Wang, X. Zhang, H. Tang, X. Liu, F. Huang, Y. Cao, *Iscience* **2019**, *13*, 33-42.

[6] S. Li, L. Ye, W. Zhao, H. Yan, B. Yang, D. Liu, W. Li, H. Ade, J. Hou, *Journal of the American Chemical Society* **2018**, *140*, 7159-7167.

[7] Y. Liu, J. Zhao, Z. Li, C. Mu, W. Ma, H. Hu, K. Jiang, H. Lin, H. Ade, H. Yan, *Nature communications* **2014**, *5*, 1-8.

[8] aF. Zhang, D. Wu, Y. Xu, X. Feng, *Journal of Materials Chemistry* **2011**, *21*, 17590-17600; bJ. Xu, W. Li, W. Liu, J. Jing, K. Zhang, L. Liu, J. Yang, E. Zhu, J. Li, Y. Zhu, *Angewandte Chemie International Edition* **2022**, *61*, e202212243; cX. Yuan, C. Wang, L. Vallan, A. T. Bui, G. Jonusauskas, N. D. McClenaghan, C. Grazon, S. Lacomme, C. Brochon, H. Remita, G. Hadziioannou, E. Cloutet, *Advanced Functional Materials*, *n/a*, 2211730.

[9] Z. Hu, B. Shao, G. T. Geberth, D. A. V. Bout, *Chemical science* **2018**, *9*, 1101-1111.

[10] aW. C. Tsoi, D. T. James, J. S. Kim, P. G. Nicholson, C. E. Murphy, D. D. Bradley, J. Nelson, J.-S. Kim, *Journal of the American Chemical Society* **2011**, *133*, 9834-9843; bJ.-H. Kim, C. E. Song, N. Shin, H. Kang, S. Wood, I.-N. Kang, B. J. Kim, B. Kim, J.-S. Kim, W. S. Shin, *ACS applied materials & interfaces* **2013**, *5*, 12820-12831; cS. Wood, J. R. Hollis, J.-S. Kim, *Journal of Physics D: Applied Physics* **2017**, *50*, 073001.

[11] aW. S. Fall, J. r. Baschnagel, O. Benzerara, O. Lhost, H. Meyer, *ACS Macro Letters* **2023**, *12*, 808-813; bZ. He, Z. Zhang, S. Bi, *Materials Advances* **2022**, *3*, 1953-1973.

[12] Y. Lin, X. Zhan, *Accounts of chemical research* **2016**, *49*, 175-183.

[13] T. Eder, T. Stangl, M. Gmelch, K. Remmerssen, D. Laux, S. Höger, J. M. Lupton, J. Vogelsang, *Nature communications* **2017**, *8*, 1-11.

[14] C. Matt, D. L. Meyer, F. Lombeck, M. Sommer, T. Biskup, *Macromolecules* **2018**, *51*, 4341-4349.

[15] aW. Huang, Y. Hu, Z. Qin, Y. Ji, X. Zhao, Y. Wu, Q. He, Y. Li, C. Zhang, J. Lu, *National Science Review* **2023**, *10*, nwac171; bX. Yuan, C. Wang, L. Vallan, A. T. Bui, G. Jonusauskas, N. D. McClenaghan, C. Grazon, S. Lacomme, C. Brochon, H. Remita, *Advanced Functional Materials* **2023**, *33*, 2211730.

Entry for the Table of Contents

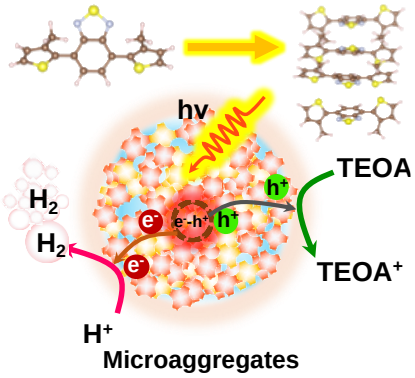

The relationship between the aggregation of TBT-based conjugated trimers and the photocatalytic activity was systematically investigated by methyl side-chain engineering. TBT-3 with the smallest size of aggregates and best crystalline, exhibit the best photocatalytic H_2 evolution activity, which is due to the shorten charge carrier transport distance and solid long-range order.